

It is well known [1, 2] that streamer-type of gas breakdown occurs under single-electrode initiation of a high-pressure discharge in discharge gaps under overvoltage. A single electron avalanche with multiplication of the number of electrons passes into the plasma state and the electric field is squeezed out to the edge of the avalanche. The ends of the streamer then propagate toward the anode and the cathode. The avalanche-streamer transition (AST) was simulated mathematically in [3-5] on the basis of the diffusion-drift approximation (DDA) in the two-dimensional case (axial symmetry was assumed). The results of the computations were contradictory. In [4], for example, the profiles of the electron and ion densities, n_e and n_i , were monotonic with one maximum and the distribution of the field E along the streamer axis had two very distinct maxima. In [5] Pavlovskii et al. observed oscillations of n_e , n_i , and E along the streamer axis, from which they concluded that instability had developed in the streamer. Since the study of AST plays a key role in understanding the mechanism of gas breakdown, it is necessary to ascertain what causes the disparity in the results [4, 5] obtained with the framework of the same mathematical model of AST. As the electric field strength increases, "runaway" electrons appear [6] and the electron distribution function (EDF) begins to depend on the electric field strength in a non-local manner. The use of DDA, therefore, may become incorrect. Below we carry out AST calculations for neon using different models. We investigate the distribution of n_e , n_i , and E along the streamer axis, the application of DDA in strong fields, and the evolution of an electron avalanche with considerable effect from electron runaway.

Mathematical Models of AST. In the AST stage electron annihilation can be ignored and electrons are created through collision ionization of atoms in the ground state. The displacement of low-mobility ions is insignificant and within the framework of the DDA the system of equations describing the streamer has the form

$$\partial n_e / \partial t - \operatorname{div}(\mu E n_e + D \operatorname{grad} n_e) = S = \alpha \mu |E| n_e; \quad (1)$$

$$\partial n_i / \partial t = S; \quad (2)$$

$$\Delta \varphi = 4\pi e(n_e - n_i), \quad \mathbf{E} = -\nabla \varphi; \quad (3)$$

where μ and D are the electron mobility and diffusion coefficient and α is Townsend's ionization coefficient of the gas. We consider a long discharge gap, when the effect of the electrodes can be ignored and primary electrons are created in the volume. Then the following initial and boundary conditions can be put into the system (1)-(3):

$$n_e|_{t=0} = n_i|_{t=0} = \delta(\mathbf{r}), \quad E_x|_{|r|\rightarrow\infty} = E_y|_{|r|\rightarrow\infty} = 0, \quad E_z|_{|r|\rightarrow\infty} = -E_0$$

(the z axis is directed from the cathode to the anode and δ is the Dirac delta function).

Since the computing time is limited, use of Eqs. (1)-(3) (model I) does not allow the streamer evolution to be tracked far enough. Davies and Evans [7] proposed a simpler model for describing a discharge, using one-dimensional transport equations

$$\frac{\partial n_i}{\partial t} = \frac{\partial n_e}{\partial t} - \frac{\partial}{\partial z} \mu E n_e - \frac{\partial}{\partial z} D \frac{\partial n_e}{\partial z} = \alpha \mu |E| n_e, \quad (4)$$

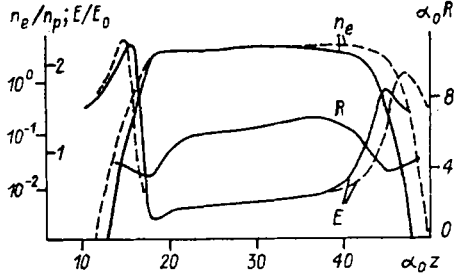


Fig. 1

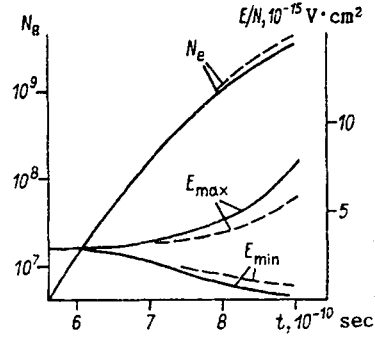


Fig. 2

and the field strength at the streamer axis is found by the method of "disks":

$$E = -E_0 + 2\pi e \int K(z-z')(n_e(z') - n_i(z')) dz',$$

$$K(z) = z/|z| - z/\sqrt{R_C^2 + z^2}. \quad (5)$$

In the derivation of Eqs. (4) and (5) (model II) it was assumed that the electron and ion density is distributed uniformly with respect to radius when $r < R_C$ and is zero when $r > R_C$. When simulating a streamer, it is natural to assume that the effective channel radius R_C is equal to the avalanche diffusion radius $R_S = \sqrt{4Dt_S}$ at the time t_S of the onset of AST: $\alpha_0 v_0 t_S \approx \ln(E_0 R_S^2 / e) \sim 20$, $\alpha_0 = \alpha(E_0)$, $v_0 = \mu E_0 [1, 2]$.

In model III the electron distribution function $f(v, r, t)$ was found by solving the kinetic equation

$$\frac{\partial f}{\partial t} + \mathbf{v} \frac{\partial f}{\partial \mathbf{r}} - \frac{e\mathbf{E}}{m} \frac{\partial f}{\partial \mathbf{v}} = st\{f\}, \quad f|_{t=0} = \delta(\mathbf{r})\delta(\mathbf{v})$$

by the Monte Carlo method. The collisional term $st\{f\}$ took into account elastic scattering, which was assumed to be isotropic with respect to angles, excitation, and ionization of neon atoms. The ensemble of real levels of neon was replaced by an effective level with excitation energy 16.6 eV [8]. The transport cross section for electron scattering was taken from [8]. The resulting electron density $n_e = \int f(v, r, t) dv$ and the collisional ionization rate $S = \int v\sigma_i f(v, r, t) dv$ were averaged over the radius R_C . The ion density and electric field strength were then determined as in model II.

Numerical Simulation Procedure. We solved the electron and ion transport equations by using an explicit monotonic conservative scheme. The diffusion term was approximated from a symmetric difference scheme with the second order of accuracy and the convective term, with the first order of accuracy from a running calculation scheme. The solution of the systems of equations (1)-(3) and (4), (5) was also found by an explicit method, i.e., first the transport equation was solved and the resulting electron and ion densities were used to determine the electric field. Poisson's equation (3) was solved by the alternating-triangular method [10] and the integral on the right-hand side of (5) was calculated by the method of trapezoids. The two-dimensional computations were carried out on a nonuniform grid. The value of the potential at the boundaries of the grid was determined as in [5], thus allowing the number of grid points to be reduced. Models II and III were studied on a uniform grid.

Since the explicit method is used virtually in all studies on numerical simulation of discharge ignition, it is necessary to analyze the limitation on τ , the maximum time interval of the computation. The limitation on τ when solving the electron transport equation is well known. For example, for the one-dimensional case

$$\tau < h/(v_{\max} + 2D/h) \quad (6)$$

(v_{\max} is the maximum electron drift velocity and h is the grid spacing with respect to the coordinate). It is precisely condition (6) which is usually employed when choosing the time interval. As the gas conductivity $\sigma = e\mu n_e$ increases, however, an additional limitation on

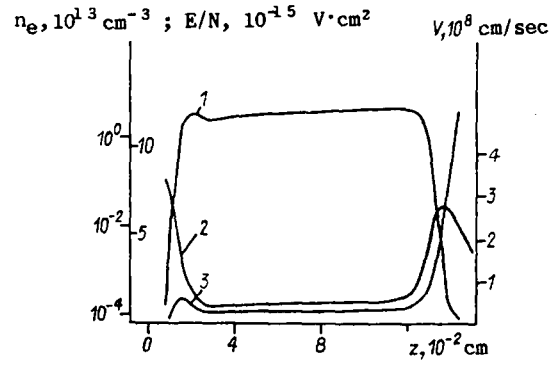


Fig. 3

τ results and this limitation may become more stringent than condition (6). We shall show this on the sample of the system of equations (1)-(3), the consequence of which is the law of conservation of current,

$$\frac{1}{4\pi} \frac{\partial \mathbf{E}}{\partial t} + \sigma \mathbf{E} + eD\nabla n_e = \mathbf{j}, \quad \text{div } \mathbf{j} = 0. \quad (7)$$

The solution of system (1)-(3) by the explicit method is equivalent to the use of the explicit scheme for the solution (7), which imposes the limitation

$$\tau < 1/4\pi\sigma_{\max} \quad (8)$$

(σ_{\max} is the maximum conductivity of the gas). The physical meaning of condition (8) is obvious: the time interval of the computation should be shorter than the minimum Maxwellian dissipation of the charge in the plasma. We should emphasize that linear analysis does not give a complete guarantee of stability when nonlinear equations are to be solved and the stability must be checked further by reducing the time interval. The experience gained from our calculations shows that nonfulfilment of condition (8) results in the appearance of field oscillations, which cause oscillations of the electron and ion density. Judging by the data on τ and σ , computational oscillations were apparently observed in the AST calculations in [5].

A Monte Carlo method for solving the kinetic equation was described in [11]. We point out only that an additional limitation $\tau\omega_p < 1$ ($\omega_p = \sqrt{4\pi e^2 n_e/m}$ is the plasma electron frequency [12]) arises in model III. The number of particles in a sphere of Debye radius $R_d = v_T/\omega_p$ (v_T is the random electron velocity) should be fairly high [12]. This substantially limits the possibility of simulating a streamer by the Monte Carlo method after AST, when R_d becomes much smaller than the streamer dimensions.

Results and Discussion. In the simulation of AST within the framework of models I and II, the values of μ and D were assumed to be field-independent and Townsend's ionization coefficient was written as $\alpha = A \exp(-\sqrt{BN/E})N$ [13] (N is the concentration of gas atoms). In dimensionless variables $\alpha_0 r$, $\alpha_0 v_0 t$, n_e/n_p , n_i/n_p , $n_p = \alpha_0 E_0 / 4\pi e$, E/E_0 , and $\alpha_0 \varphi/E_0$ the behavior of the streamer is determined by the values of the parameters $\alpha_0 R_S$ and BN/E_0 and depends weakly on N . A change in N leads only to a shift of the time when AST occurs, $t_S(N_0) - t_S(N_1) = \ln(N_1/N_0)/\alpha_0 v_0$, and causes a slight change in $\alpha_0 R_S$. Below we assume that $N = 10^{19} \text{ cm}^{-3}$. A typical distribution of the parameters (along the axis of the streamer) n_e and E and the effective streamer radius $R = \sqrt{2 \int n_e(z, r) r dr / n_e(r, z=0)}$ for $\alpha_0 v_0 t = 22.3$, $\alpha_0 R_C = 4.4$, and $BN/E_0 = 1.68$ are shown in Fig. 1 (the solid line represents model I, the dashed line represents model II). In contrast to the case at low overvoltages [4], the maximum electric field strength is attained at the cathode end of the streamer. Despite the variation of the streamer radius during AST, there is good agreement between models I and II. This justifies the use of the economical model II for calculations of AST and subsequent streamer evolution, which have been carried out in a number of studies [14, 15]. Good agreement between the results from model II and the data from two-dimensional calculations of AST in nitrogen is also obtained for substantially lower overvoltages [4]. Since AST has been considered in a fairly detailed

manner in [3, 4], we shall only point out here that the characteristic profile of the field and the electron density persists as the streamer develops further.

For comparison of models II and III the values of μ , D , and α were given as an approximation of the results found by calculating the EDF in a uniform field. In this regard, we should mention that the Monte Carlo results coincide with data from the finite-difference solution of the kinetic equation, which were found in [16, 17] using an identical set of cross sections. The time dependence of the total number N_e of electrons, the maximum and minimum field strengths E_{\max} and E_{\min} at $E_0/N = 283 \cdot 10^{-17} \text{ V} \cdot \text{cm}^2$, and $R_C = 1.56 \cdot 10^{-2} \text{ cm}$ is shown in Fig. 2 (the dashed lines represent model II and the solid lines, model III). At low overvoltages the total number of electrons in an avalanche is observed to increase, at first subexponentially and then superexponentially [4]. For high overvoltages the distortion of the electric field during AST always leads to a subexponential growth of N_e , this being associated with saturation of the ionization coefficient of the gas. There is good quantitative as well as qualitative agreement between the DDA and the kinetic model. The profiles of the electron density and the field strength (lines 1, 2), obtained with the kinetic model (Fig. 3, $E_0/N = 283 \cdot 10^{-17} \text{ V} \cdot \text{cm}^2$, $t = 8.9 \cdot 10^{-10} \text{ sec}$, line 3 is the velocity of the directed motion of electrons), are also in agreement with the data of models I and II. High-energy electrons, which should in principle affect the mechanism of propagation of the anode-directed streamer, appear at the anode end of the streamer. Calculations of the streamer evolution within the framework of the kinetic model, carried out in [18] with allowance for volume photoionization of the gas, show that photoionization plays a more important role. The concept of the formation of plasma oscillations was invoked in [19-21] to explain the mechanism of AST and the further development of the streamer. In contrast to the DDA, the kinetic model did allow the possibility of plasma oscillations building up. The results of calculations in the range of parameter variation studied, however, did not reveal development of instability and generation of plasma oscillations in the AST stage.

We note that when the Monte Carlo method is used, oscillations in the behavior of the streamer characteristics arise, especially in the range of high conductivity. Figures 2 and 3 show smooth curves, since the oscillation evidently lies within the limits of the statistical error of the Monte Carlo method.

An increase in the field leads to a qualitative change in the avalanche evolution at $E_0/N \gtrsim 10^{-14} \text{ V} \cdot \text{cm}^2$. The behavior of the energy U and the velocity w of directed motion of an individual electron is described by the equations [22]

$$\partial w / \partial t = -eE/m - N\sigma_{tr}vw; \quad (9)$$

$$\partial U / \partial t = -ewE - N\beta v, \quad v = \sqrt{2U/m}. \quad (10)$$

Since the transport cross section σ_{tr} and the energy loss $N\beta$ per unit length, starting from a certain threshold, decrease with increasing energy, at $E_0 > E_x$ the electrons pass into a runaway regime, i.e., a regime of continuous acquisition of energy. If we set $w = -vE/|E|$ in (10), then from that equation we can find an estimate for the runaway field $E_* \approx E_1 = N \max_U \beta(U)/e$, and this estimate is usually employed [23, 24]. If we start from the complete system of equations (9) and (10), then we obtain the estimate $E_* \approx E_2 = N \max_U 2U\beta(U)\sigma_{tr}$, which judging by EDF calculations, corresponds more to the determination of the runaway field. For neon, $E_1/N \approx 4.1 \cdot 10^{-15} \text{ V} \cdot \text{cm}^2$ and $E_2/N \approx 1.2 \cdot 10^{-14} \text{ V} \cdot \text{cm}^2$.

Because of the random nature of the scattering processes, part of the electrons pass into the runaway regime at $E_0 \lesssim E_1$ as well, but their fraction is small and rapidly decreases with decreasing E_0 . In fields close to E_1 , therefore, no particular qualitative changes in the AST mechanism are observed. At $E_0 \gtrsim E_2$, because of the creation of secondary electrons the "body" of the EDF the average electron energy, α , and other characteristics of the EDF virtually do not vary with time but a growing "tail" of high-energy electrons forms in the EDF [25]. The distribution of the electron density in a single avalanche is not described, even qualitatively, within the framework of DDA, viz., the avalanche becomes markedly asymmetric; a precursor appears, consisting of runaway electrons and moving with increasing velocity [Fig. 4, $E_0/N = 1.698 \cdot 10^{-14} \text{ V} \cdot \text{cm}^2$, lines 1-4 for $t = 1.43 \cdot 10^{-11}$, $2.38 \cdot 10^{-11}$, $3.33 \cdot 10^{-11} \text{ sec}$, 1-3) electron density, 4) effective avalanche radius]. The beam of runaway electrons ionizes the gas in a filament of length $\ell \approx eE_0 t^2 / 2m$ and the radius of the filament is determined by transverse diffusion and is substantially smaller than ℓ . In strong fields primary electrons are usually created at the cathode [24]. In this case the cathode end of the avalanche is virtually not displayed from the cathode. The characteristic time t_* , starting from which the electric field is distorted by the space charge of the

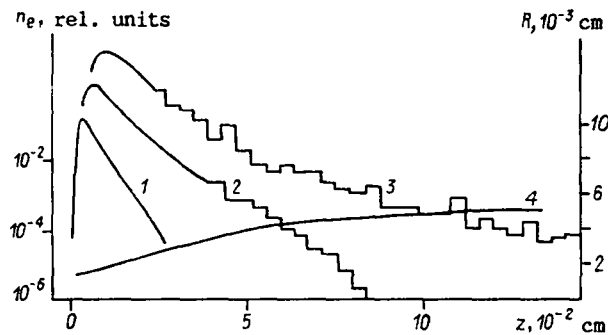


Fig. 4

avalanche, can be evaluated as $t_* \approx t_S \approx (20-30)/\alpha_0 v_0$. At $E_0 \approx E_2$ and $t \approx t_*$ the characteristic length of a filament in neon, $Nl \approx (2-4) \cdot 10^{20} \text{ cm}^{-2}$ is comparable with, or exceeds, the interelectrode separation customarily used. Accordingly, even during the development of a single avalanche in a uniform field the discharge gap is bridged by the ionized filament. Further development of the discharge should be determined by the propagation of fast ionization waves, which equalize the conductivity of the gas in the filament. A more detailed study of the evolution of electron avalanches and the mechanism of gas breakdown at $E_0 \geq E_2$ falls outside the scope of this paper.

LITERATURE CITED

1. G. Reter, *Electron Avalanches and Breakdown in Gases* [Russian translation], Mir, Moscow (1968).
2. E. D. Lozanskii, "Development of electron avalanches and streamers," *Usp. Fiz. Nauk*, **117**, No. 2 (1975).
3. V. V. Kremnev, G. A. Mesyats, and Yu. B. Yankelevich, "Development of a single electron avalanche in a gas in the nanosecond range," *Izv. Vyssh. Uchebn. Zaved., Fiz.*, No. 2 (1970).
4. I. M. Bortnik, I. I. Kochetov, and K. N. Ul'yanov, "Mathematical model of avalanche-streamer transition," *Teplofiz. Vys. Temp.*, **20**, No. 1 (1982).
5. A. I. Pavlovskii, L. P. Babich, et al., "Structure of an electron avalanche at high E/p ," *Dokl. Akad. Nauk SSSR*, **266**, No. 4 (1982).
6. A. V. Gurevich, "Contribution to the theory of the runaway electron effect," *Zh. Éksp. Teor. Fiz.*, **39**, No. 5 (1960).
7. A. I. Davies and C. J. Evans, "Field distortion in gaseous discharges between parallel-plane electrodes," *Proc. IEEE*, **114**, No. 10 (1967).
8. W. R. L. Thomas, "The determination of the total excitation cross section in neon by comparison of theoretical and experimental values of Townsend's primary ionization coefficient," *J. Phys. B*, **2**, No. 5 (1969).
9. D. Rapp and P. Englander-Golden, "Total cross sections for ionization and attachment in gas by electron impact. I. Positive ionization," *J. Chem. Phys.*, **43**, No. 5 (1965).
10. A. A. Samarskii and E. S. Nikolaev, *Methods of Solving Net Equations* [in Russian], Nauka, Moscow (1978).
11. P. Segur, M. Yousfi, et al., "The microscopic treatment of nonequilibrium regions in a weakly ionized gas," in: *Electrical Breakdown and Discharges in Gases*, Proc. NATO Adv. Study Inst., Plenum Press, New York (1983).
12. A. S. Roshal', *Simulation of Charged Beams* [in Russian], Atomizdat, Moscow (1979).
13. A. L. Ward, "Calculations of cathode-fall characteristics," *J. Appl. Phys.*, **33**, No. 9 (1962).
14. W. Reininghaus, "Calculations of streamers in gaseous discharges," *J. Phys. D*, **6**, No. 12 (1973).
15. L. E. Kline, "Calculations of discharge initiation in overvolted parallel-plane gaps," *J. Appl. Phys.*, **45**, No. 5 (1974).
16. K. Kitamory, H. Tagashira, and Y. Sakai, "Relaxation processes of the electron velocity distributions in neon," *J. Phys. D*, **11**, No. 3 (1978).
17. A. G. Ponomarenko, V. N. Tishchenko, and V. A. Shveigert, "Relaxation of electron distribution function in a weakly ionized neon plasma," *Fiz. Plazmy*, **11**, No. 4 (1985).

18. V. Tzeng and E. E. Kundhart, "New insight into streamer development," Fourth IEEE Pulsed Power Conference, New York (1983).
19. N. S. Rudenko and V. I. Smetanin, "Mechanism of propagation of streamers on the basis of plasma oscillations," *Izv. Vyssh. Uchebn. Zaved., Fiz.*, No. 7 (1977).
20. O. A. Omarov, M. B. Khachalov, et al., "Formation of a spark channel," *Fiz. Plazmy*, 4, No. 2 (1978).
21. L. P. Babich, "Role of plasma waves in the spark breakdown of gases," *Fiz. Plazmy*, 7, No. 6 (1981).
22. V. P. Ginzburg and A. V. Gurevich, "Nonlinear phenomena in plasma in an alternating electric field," *Usp. Fiz. Nauk*, 10, No. 2 (1960).
23. L. P. Babich and Yu. L. Stankevich, "Criterion for the transition from a streamer mechanism of discharge to continuous electron acceleration," *Zh. Tekh. Fiz.*, 42, No. 8 (1972).
24. G. A. Mesyats, Yu. I. Bychkov, and V. V. Kremnev, "Pulsed nanosecond electrical discharge in a gas," *Usp. Fiz. Nauk*, 107, No. 2 (1972).
25. G. V. Gadiyak, K. A. Nasyrov, et al., "Mathematical simulation of gas-discharge lasers," Preprint [in Russian], *Inst. Teor. Prikl. Mekh. Sib. Otd. Akad. Nauk SSSR*, No. 30-85, Novosibirsk (1985).

MODEL OF A STREAMER IN A LONG DISCHARGE GAP

V. P. Meleshko and V. A. Shveigert

UDC 537.521

Detailed experimental data have been published on the development of a streamer with characteristic times substantially longer than the avalanche-streamer transition (AST) time. The results of the different experiments are not completely consistent even at the qualitative level. Rudenko and Smetanin [1] and Davidenko et al. [2], observing that a streamer formed at the center of a discharge gap and propagated toward the electrodes, determined that the velocity of both ends of the streamer increases rapidly and continuously. Bayle et al. [3] found that the streamer velocity became saturated as the channel moved through a long discharge gap. The contradiction is not resolved by the results of other experimental studies. Kline [4], Reininghaus [5], and Dhali and Williams [6] carried out calculations of a streamer in the diffusion-drift approximation. However, they studied only the initial stage in the formation of the streamer channel, which does not indicate the nature of the channel development in a long discharge gap at long characteristic times. The development of a long streamer is described only phenomenologically by existing models [7, 8].

In this study, in the diffusion-drift approximation we numerically simulate the development of a streamer in neon under one-electrode initiation of a discharge at the center of the gap with the gas at atmospheric pressure. The gap was assumed to be unbounded and the effect of the electrodes was not taken into account. The streamer channel was calculated to grow to a length of up to 7 cm. Two phases were shown to exist in the development of the streamer: an acceleration phase, when the velocity of the streamer increases rapidly; and a phase of quasi-steady development, in which case the streamer velocity changes very slowly.

The two-dimensional calculation of streamer development over a long time requires much computer time. Accordingly, a one-dimensional model is used to calculate the transport of charged particles. The initial stage of streamer development has already been calculated in such a model [4].

The behavior of electrons and ions is described by the equations

$$\frac{\partial n_e}{\partial t} + \mu_e \frac{\partial n_e E}{\partial x} = D_e \frac{\partial^2 n_e}{\partial x^2} + \alpha n_e \mu_e E - \beta n_e n_i + \frac{n^*}{\tau_{ac}},$$

$$\frac{\partial n_i}{\partial t} = \alpha n_e \mu_e E - \beta n_e n_i + \frac{n^*}{\tau_{ac}},$$